

PPP2R2D suppresses interleukin-2 production and regulatory T cell function

Wenliang Pan, ... , Maria G. Tsokos, George C. Tsokos

JCI Insight. 2020. <https://doi.org/10.1172/jci.insight.138215>.

Research In-Press Preview Immunology

Protein phosphatase 2A is a ubiquitously expressed serine/threonine phosphatase which comprises a scaffold, a catalytic and multiple regulatory subunits and has been shown to be important in the expression of autoimmunity. We considered that a distinct subunit may account for the decreased production of interleukin-2 (IL-2) in people and mice with systemic autoimmunity. We show that the regulatory subunit PPP2R2D is increased in T cells from people with systemic lupus erythematosus and regulates IL-2 production. Mice lacking PPP2R2D only in T cells produce more IL-2 because the IL-2 gene and genes coding for IL-2 enhancing transcription factors remain open and the levels of the enhancer phosphorylated CREB are high. Mice with T cell-specific PPP2R2D deficiency display less systemic autoimmunity when exposed to a TLR7 stimulator. While genes related to regulatory T cell function do not change in the absence of PPP2R2D, regulatory T cells exhibit high suppressive function *in vitro* and *in vivo*. Because the ubiquitous expression of protein phosphatase 2A cannot permit systemic therapeutic manipulation, the identification of regulatory subunits able to control specific T cell functions opens the way for the development of novel, function-specific drugs.

Find the latest version:

<https://jci.me/138215/pdf>



PPP2R2D suppresses interleukin-2 production and regulatory T cell function.

Wenliang Pan¹, Amir Sharabi¹, Andrew Ferretti¹, Yinfeng Zhang², Catalina Burbano¹, Nobuya Yoshida¹, Maria G. Tsokos¹, George C. Tsokos^{1*}

¹Department of Medicine, Beth Israel Deaconess Medical Center and Harvard Medical School, Boston, MA

² Department of Pathology, John Hopkins University School of Medicine, Baltimore, MD

Conflict of interest statement

The authors have declared that no conflict of interest exists

*Address correspondence to GCT:

3 Blackfan Circle, CLS-937,

Boston, MA 02215, USA.

Phone: +1 617-735-4160

Email: gtsokos@bidmc.harvard.edu

Abstract

Protein phosphatase 2A is a ubiquitously expressed serine/threonine phosphatase which comprises a scaffold, a catalytic and multiple regulatory subunits and has been shown to be important in the expression of autoimmunity. We considered that a distinct subunit may account for the decreased production of interleukin-2 (IL-2) in people and mice with systemic autoimmunity. We show that the regulatory subunit PPP2R2D is increased in T cells from people with systemic lupus erythematosus and regulates IL-2 production. Mice lacking PPP2R2D only in T cells produce more IL-2 because the *IL-2* gene and genes coding for IL-2 enhancing transcription factors remain open and the levels of the enhancer phosphorylated CREB are high. Mice with T cell-specific PPP2R2D deficiency display less systemic autoimmunity when exposed to a TLR7 stimulator. While genes related to regulatory T cell function do not change in the absence of PPP2R2D, regulatory T cells exhibit high suppressive function *in vitro* and *in vivo*. Because the ubiquitous expression of protein phosphatase 2A cannot permit systemic therapeutic manipulation, the identification of regulatory subunits able to control specific T cell functions opens the way for the development of novel, function-specific drugs.

Introduction

Systemic lupus erythematosus (SLE) is an autoimmune disease with a complex pathogenesis. The expression of autoimmunity and organ inflammation involves altered production of cytokines by T cells (1-3). Specifically, decreased IL-2 production may account for the reported decreased cytotoxic T cell function and the decreased function and numbers of regulatory T (T_{reg}) cells (2), whereas increased production of IFN- γ and IL-17 may contribute directly to organ inflammation (4, 5). Treatment with low doses of IL-2 diminishes renal inflammation and the rate of kidney-infiltrating CD4⁺ T cells in murine lupus nephritis (6). Low-dose of IL-2 in the treatment of autoimmune diseases including SLE, rheumatoid arthritis, and multiple sclerosis is in clinical trials (7). IL-2 is a pleiotropic cytokine produced by effector T (T_{eff}) cells after antigen activation and is at the crossroads of effector responses, tolerance, and immunotherapy (8). IL-2 transcription is mediated by multiple transcription factors, including activator protein-1 (AP-1, FOS-JUN family dimers), cAMP responsive element binding protein (CREB), nuclear factor of activated T cells (NFAT) family proteins, nuclear factor κ -light-chain-enhancer of activated B cells (NF- κ B), ETS-related transcription factor (Elf1) and GA binding protein alpha chain (GABPA) (9). T_{reg} cells have abundant expression of the IL-2 receptor α -chain (CD25) but are unable to produce IL-2. IL-2 binds with low affinity to CD25 or to heterodimers of the common γ -chain (CD132) and IL-2R β (CD122), but receptor affinity increases \sim 1,000-fold when these subunits collectively interact with IL-2 (10). Capture of IL-2 by T_{reg} cells is critical for their suppressor function and limiting the activation of T cells (11).

Protein phosphatase 2A (PP2A) is a ubiquitously expressed and highly conserved serine/threonine phosphatase that is important in multiple cellular processes including cell division, cytoskeletal dynamics and various signaling pathways (12). The PP2A core enzyme consists of the scaffold subunit A (PP2A_A) and the catalytic subunit C (PP2A_C). To form a functional holoenzyme, the core enzyme interacts with one of the many regulatory subunits (PP2A_B), which define substrate and tissue specificity (13). The regulatory subunits are classified into four major families, identified as B (e.g. PPP2R2A, PPP2R2B, PPP2R2C and PPP2R2D), B' (PPP2R5A, PPP2R5B, PPP2R5C, PPP2R5D and PPP2R5E), B'' (PPP2R3A, PPP2R3B and PPP2R3C) and B''' (striatin/PR93) (13). We have previously shown that PP2A mRNA, protein and catalytic activity are increased in T cells from patients with SLE and that PP2A_C is responsible for the dephosphorylation of transcriptional enhancer CREB which contributes to decreased IL-2 production (14, 15). Although silencing PP2A_C or inhibition of its activity increases IL-2 production in T cells (16), in subsequent studies we found that PP2A_C is requisite for T_{reg} cell function (17) and enables IL-2 signaling during T_{reg} development (18).

These apparently contradictory effects make PP2Ac inhibitors unlikely to be used for treatment of patients with SLE. However, we previously showed that the PP2A regulatory subunit B β (PPP2R2B) is decreased in SLE T cells and accounts for the decreased IL-2 deprivation-induced T-cell apoptosis (19). Since the specificity of PP2A function is governed by its use of a particular regulatory subunit (13) we considered that one of the regulatory subunits controls the production of IL-2 in T cells.

We have identified PPP2R2D, a regulatory subunit of PP2A, to regulate negatively IL-2 production in conventional T (T_{conv}) cells by controlling chromatin opening of the *IL-2* gene and of genes of multiple transcription factors which favor IL-2 transcription. PPP2R2D is increased in T cells from patients with SLE and mice lacking this subunit in T cells develop less autoimmunity. The linkage of PP2A regulatory subunits to specific immune cell functions should enable the development of drugs with higher clinical efficacy.

Results

PPP2R2D expression is increased in human T cells following TCR stimulation and suppresses IL-2 production

Having previously shown that PPP2R2B promotes IL-2 deprivation-induced T cell apoptosis in human T cells (20), we considered that other subunits may control directly the production of IL-2 by T cells. To this end, we determined mRNA expression of several PP2A regulatory subunits in T cells from healthy donors following T cell stimulation with CD3 and CD28 antibodies. mRNA expression increased within 30 minutes for all tested subunits except for PPP2R2B but the levels of PPP2R2D increased the most; within 24 hours mRNA levels for all tested subunits returned to normal (**Figure 1A**). We looked closely at the kinetics of expression of PPP2R2D mRNA and compared them to those of IL-2. As shown in **Figure 1B**, PPP2R2D mRNA expression increased at 30 minutes, decreased subsequently at 2 and 6 hours, increased at 12 hours, and decreased at 24 hours, while IL-2 mRNA increased at 2 hours and gradually **decreased** at 6, 12 and 24 hours. Because PP2A dephosphorylates CREB, a main transcriptional enhancer of IL-2 production, we determined the protein levels of PPP2R2D over time along with those of phosphorylated CREB (p-CREB), total CREB, and β -actin in lysates extracted from stimulated T cells at various time points. Protein levels of PPP2R2D decreased at 6 hours, and subsequently increased at 12 and 24 hours, while the ratio of p-CREB/total CREB increased at 6 hours, and subsequently decreased at 12 and 24 hours (**Figure 1, C and D**).

In order to establish the observed inverse correlation between IL-2 and PPP2R2D expression, we measured IL-2 production following stimulation of T cells in which the expression of PPP2R2D was either silenced (**Figure 1E**) or overexpressed (**Figure 1F**). Within 6 hours after stimulation IL-2 production increased significantly in CD4 T cells (10-fold higher compared with baseline). When PPP2R2D was silenced the frequency of IL-2-producing CD4 T cells increased further at 6 hours, and decreased slowly at 12 and 24 hours after stimulation (**Figure 1E**). In contrast, PPP2R2D overexpression prevented the induction of IL-2-producing CD4 T cells in response to CD3/CD28 stimulation at all tested time points (**Figure 1F**). It is noteworthy that neither silencing nor overexpression of PPP2R2D in T cells affected significantly the frequency of IFN- γ - and IL-4-producing CD4 T cells in response to CD3/CD28 stimulation (**Supplemental Figure 1, A and B**). These experiments reveal an important and specific role of PPP2R2D in the production of IL-2.

PPP2R2D expression is increased in T cells from patients with SLE

T cells for patients with SLE display high levels of PP2A which has been linked to decreased IL-2 production. Having shown that PPP2R2D suppressed the production of IL-2 we sought to determine the expression levels of PPP2R2D in SLE T cells. We found that fresh unstimulated T cells from patients with SLE express high levels of PPP2R2D mRNA compared to T cells from healthy controls (Table 1, **Figure 2A**). In parallel to mRNA, the expression of PPP2R2D protein was found increased in T cell lysates from patients with SLE compared to healthy controls (representative Western blots for PPP2R2D and β -actin are shown in **Figure 2B** and cumulative data are shown in **Figure 2C**). However, we did not find a correlation between PPP2R2D expression in SLE T cells and Systemic Lupus Erythematosus Disease Activity Index (SLEDAI) (**Figure 2D**).

PPP2R2D deficiency in T cells promotes chromatin remodeling of the IL-2 locus

To address the function of PPP2R2D in T cells in a definitive manner, we generated C57BL/6J mice in which exon 6 of *PPP2R2D* gene is flanked by loxP ($R2D^{fl/fl}$ mice) using CRISPR/Cas9 technology (**Supplemental Figure 2A**), as previously described (21). Excision of exon 6 was confirmed by *in vitro* Cre recombination of PCR products amplified from candidate founders (**Supplemental Figure 2B**). We then crossed these mice with Lck^{cre} mice to generate conditional knockout mice ($Lck^{cre}R2D^{fl/fl}$) where PPP2R2D deletion was limited to T cells (**Supplemental Figure 2C**).

We next determined the role of PPP2R2D in T cell development in $R2D^{fl/fl}$ and $Lck^{cre}R2D^{fl/fl}$ mice. As shown in **Supplemental Figure 3, A-C**, there were no significant differences in the percentage and absolute numbers of T cell subsets in the thymus from $R2D^{fl/fl}$ and $Lck^{cre}R2D^{fl/fl}$ mice. In order to determine the effect of PPP2R2D deficiency in the survival of thymocytes, we used a CD3 antibody to stimulate thymocytes imitating TCR stimulation during double positive (DP) cell development. Thymocytes isolated from $R2D^{fl/fl}$ and $Lck^{cre}R2D^{fl/fl}$ mice were stimulated with CD3 antibody overnight and stained for Annexin V expression. As shown in **Supplemental Figure 3, D-F**, CD3 antibody stimulation produced a similar percentage of apoptotic double negative (DN) or DP cells in $R2D^{fl/fl}$ and $Lck^{cre}R2D^{fl/fl}$ thymocytes. Furthermore, there were no significant differences in the percentage and absolute numbers of T cell subsets in spleens from $R2D^{fl/fl}$ and $Lck^{cre}R2D^{fl/fl}$ mice (**Supplemental Figure 3, G-I**). These results suggested that PPP2R2D deficiency in T

cells does not impair T cell development in the thymus and T cell subset distribution in the spleen.

To determine how PPP2R2D regulates T cell signaling at the level of genome-wide transcriptional profile, we performed an assay for transposase accessible chromatin using sequencing (ATAC-seq) in CD4 T_{conv} cells (Thy1.2⁺CD4⁺CD25^{lo}CD127^{lo}) which were sorted by flow cytometry from spleens of R2D^{fl/fl} or Lck^{cre}R2D^{fl/fl} mice and stimulated *in vitro* by plate bound CD3 and CD28 antibodies for 4 hours. Heatmap clustering of Pearson correlation coefficients revealed a strong correlation between replicates of the same condition in chromatin accessibility, but a weaker correlation in profile between R2D^{fl/fl} (wild-type) and Lck^{cre}R2D^{fl/fl} (PPP2R2D KO) T_{conv} cells (**Figure 3A**). We next examined the genomic distribution of ATAC-seq open chromatin peaks. As shown in **Figure 3B**, a large proportion of ATAC-seq peaks are located close to the transcription start site (TSS), and the number of peaks in Lck^{cre}R2D^{fl/fl} T_{conv} cells was higher than those in R2D^{fl/fl} T_{conv} cells. In order to identify the sites of differential accessibility between R2D^{fl/fl} and Lck^{cre}R2D^{fl/fl} T_{conv} cells we performed analysis using DESeq2 as previously described (22). Using 2-fold log₂ difference and false discovery rate (FDR) less than or equal to 0.01 as cutoff, we found a larger number of sites differentially open in Lck^{cre}R2D^{fl/fl} T_{conv} as compared to R2D^{fl/fl} T_{conv} cells (**Supplemental Table 1, Figure 3C**). To further associate these differentially open sites with the transcription factor (TF) networks, we calculated the enrichment of TF-binding motifs at sites that significantly differed in accessibility, using HOMER (Hypergeometric Optimization of Motif EnRichment). At peaks more open in Lck^{cre}R2D^{fl/fl} T_{conv} cells, we found motifs for several members of the ETS (e.g. Fli1, Elf1, GABPA and ETS1), bzip (e.g. Fos, AP1, FRA2 and CREB1), RHD (e.g. NFAT and NFkB-p65-Rel) and Runt (e.g. Runx and ETS-Runx) families to be most significantly enriched (**Figure 3D**). Interestingly, most of these TFs are centered on IL-2 whose transcription is mediated by multiple transcription factors, including activator protein-1 (AP-1, FOS-JUN family dimers), CREB, NFAT family proteins, NF-κB, Elf1 and GABPA (9). Furthermore, sequencing read densities at genes encoding *IL-2* and its related TFs, such as *Jun*, *Fos*, *Nfatc1*, *Nfkb1* and *Rela* were increased in Lck^{cre}R2D^{fl/fl} T_{conv} cells in comparison to those in R2D^{fl/fl} T cells (**Figure 3E**), demonstrating that lack of PPP2R2D expression promoted the chromatin accessibility of IL-2 and its related TFs.

PPP2R2D deficiency enhances IL-2 production in T cells

In order to confirm the above-mentioned findings, R2D^{fl/fl} and Lck^{cre}R2D^{fl/fl} spleen CD4 or CD8 T cells were stimulated *in vitro* with phorbol myristate acetate (PMA) /ionomycin, and brefeldin A

for 4 hours prior to staining for intracellular cytokines followed by fluorescence-activated cell sorting (FACS) analysis. In line with ATAC-seq results, PMA/ionomycin induced higher percentage of IL-2-producing cells (**Figure 4, A and B**) and expression levels of IL-2 (**Figure 4C**) in both Lck^{cre}R2D^{fl/fl} CD4 and CD8 T cells compared to those in R2D^{fl/fl} T cells. However, there was no significant difference in the percentage of IFN- γ -producing cells and the expression level of IFN- γ in both CD4 and CD8 T cells from Lck^{cre}R2D^{fl/fl} and R2D^{fl/fl} mice following PMA/ionomycin stimulation (**Supplemental Figure 4, A-C**), which is in agreement with our findings in human T cells. In addition, lack of PPP2R2D expression did not affect the *in vitro* differentiation of CD4 naïve T cells into either T-helper cells Th1 and Th17 or T_{reg} cells (**Supplemental Figure 4, D-F**). Next we investigated the transcription of IL-2 and found that following stimulation with CD3 and CD8 antibodies Lck^{cre}R2D^{fl/fl} CD4 T cells displayed more IL-2 mRNA levels (**Figure 4D**) and promoter activity (**Figure 4E**) compared with R2D^{fl/fl} CD4 T cells. CREB is an important regulator of IL-2 transcription. Phosphorylated CREB at Ser133 residue enhances the activity of the IL-2 promoter through direct binding to the -180 site of the IL-2 promoter (23), or by upregulating the expression of other IL-2 transcription factors cJUN, cFOS, FRA2 and FOSB (9). Our previous data showed that PP2A is able to dephosphorylate CREB (16), thus we interrogated whether PPP2R2D, the regulatory subunit of PP2A, is involved in this process. Notably, Western blot analysis showed that PPP2R2D-deficient (Lck^{cre}R2D^{fl/fl}) CD4 T cells displayed increased pCREB levels (**Figure 4F**) in comparison to wild-type (R2D^{fl/fl}) CD4 T cells. This is probably caused by the decreased binding of PP2A catalytic subunit C (PP2Ac) to CREB in the absence of the regulatory subunit PPP2R2D (**Figure 4G**). These results suggest that PPP2R2D deficiency is involved in the maintenance of pCREB, which along with the aforementioned opening of a number of IL-2 transcriptional enhancers augments IL-2 production.

PPP2R2D deficiency in T cells alleviates imiquimod-induced lupus-like pathology in mice

IL-2 production is deficient in the T cells of patients with SLE (2), and treatment with low doses of IL-2 diminishes disease activity by promoting T_{reg} cell function (7). To determine the role of PPP2R2D-deficient T cells in regulation of lupus-related pathology, we applied imiquimod, a TLR7 stimulator, to the skin of ear of 8-week-old R2D^{fl/fl} and Lck^{cre}R2D^{fl/fl} mice to induce lupus-like disease, as previously described (24). As shown in **Figure 5A**, imiquimod-treated Lck^{cre}R2D^{fl/fl} mice showed significantly reduced size and weight of spleens as compared to imiquimod-treated R2D^{fl/fl} mice. The percentage of IFN- γ - (CD3⁺CD4⁺IFN- γ ⁺ and CD3⁺CD8⁺IFN- γ ⁺; **Figure 5B and Supplemental Figure 5A**) and IL-17A- (CD3⁺CD4⁺IL-17A⁺ and CD3⁺CD8⁺IL-

17A⁺; **Figure 5C and Supplemental Figure 5B**) producing cells were significantly decreased in the imiquimod-treated Lck^{cre}R2D^{fl/fl} mice as compared to imiquimod-treated R2D^{fl/fl} mice. In contrast, the percentage of IL-2-producing cells (CD3⁺CD4⁺IL-2⁺; **Figure 5D**) and of the CD3⁺CD4⁺FoxP3⁺ cells (T_{reg} cells, **Figure 5E**) was significantly increased in the imiquimod-treated Lck^{cre}R2D^{fl/fl} mice in comparison to imiquimod-treated R2D^{fl/fl} mice. Interestingly, the expression levels of T_{reg} cell markers CD25, CTLA-4 and GITR were increased in imiquimod-treated Lck^{cre}R2D^{fl/fl} T_{reg} cells compared to the imiquimod-treated R2D^{fl/fl} T_{reg} cells (**Supplemental Figure 5C and Figure 5, F and G**). Moreover, imiquimod-treated Lck^{cre}R2D^{fl/fl} mice developed less lupus-like nephritis as evidenced by the decreased anti-dsDNA IgG levels in the serum (**Figure 5H**), proteinuria (**Figure 5I**), deposition of complement 3 and IgG in glomeruli (**Figure 5, J and K; Supplemental Figure 5D**), histologic signs of glomerulonephritis (**Figure 5, L and M**) and number of kidney-infiltrating lymphocytes (**Figure 5N**) when compared with those in the imiquimod-treated R2D^{fl/fl} mice. Collectively, PPP2R2D deficiency in T cells protects against lupus-like disease in mice.

PPP2R2D deficiency in T cells potentiates the function of T_{reg} cells

Our aforementioned findings that the percentage of T_{reg} cells in the spleens (imiquimod-induced lupus-like disease model, **Figure 5E**) were increased in Lck^{cre}R2D^{fl/fl} as compared to R2D^{fl/fl} mice raised the question whether lack of PPP2R2D expression in T_{reg} cells affects the expression of genes responsible directly for their function. To test this possibility, we performed ATAC-seq analysis of T_{reg} cells (Thy1.2⁺CD4⁺CD25^{hi}CD127^{lo}) which were isolated from spleens of R2D^{fl/fl} or Lck^{cre}R2D^{fl/fl} mice by flow cytometry, and stimulated *in vitro* with IL-2 and plate bound CD3 and CD28 antibodies for 4 hours. As shown in **Supplemental Figure 6A**, a large proportion of ATAC-seq peaks are located close to TSS, and the number of peaks in Lck^{cre}R2D^{fl/fl} T cells is similar to those in R2D^{fl/fl} T cells. Using p-value less than or equal to 0.05 as cutoff, differential accessibility analysis revealed limited sites (genes) differentially open between Lck^{cre}R2D^{fl/fl} and R2D^{fl/fl} T_{reg} cells (**Supplemental Figure 6B**). None of these genes (*Tcstv3*, *Mir101c*, *Cldn14*, *Lrrc4c*, *Gm5458*, *Vmn2r123*, *Lrrc4c*, *Cr2*, and *Nkx2-6*) are known to be involved in the suppressive function of T_{reg} cells, indicating that PPP2R2D deficiency in T_{reg} cells does not affect the expression of genes known to account for their suppressive function. These findings demonstrate that PPP2R2D controls the expression of genes related to the expression of IL-2 and the *Il-2* gene itself without affecting the expression of genes known to define T_{reg} function. Instead, we considered that the increased levels of IL-2 potentiate the suppressive function of T_{reg} cells. Indeed, PPP2R2D-deficient (Lck^{cre}R2D^{fl/fl}) T_{reg} cells displayed

more suppressive effect on the proliferation of PPP2R2D-deficient CD4 or CD8 T_{conv} cells (**Figure 6, A-D**) and the expression of IFN- γ by these cells (**Figure 6, E-G**) when compared with the suppressive effect of wild-type (R2D^{fl/fl}) T_{reg} cells.

Discussion

We present evidence that PPP2R2D, a regulatory subunit of PP2A, negatively regulates IL-2 production in T_{conv} cells by controlling chromatin opening of *IL-2* and related multiple transcription factors which enhance *IL-2* transcription. Mechanistically, we demonstrate that PPP2R2D deficiency in T cells potentiates the suppressive function of T_{reg} cells. At the translational level we show that PPP2R2D deficiency in T cells alleviates imiquimod-induced lupus-like pathology.

SLE is an autoimmune disorder of unknown etiology characterized by diverse T_{eff} cell dysfunction involving both CD4⁺ and CD8⁺ cells (1-3). Specifically, decreased IL-2 production accounts for the reported decreased cytotoxic T cell function and the decreased function and numbers of T_{reg} cells (2), whereas increased production of IFN- γ and IL-17 may contribute directly to organ inflammation (4, 5). We have previously established that the catalytic subunit PP2Ac of PP2A is increased in T cells isolated from patients with SLE and causes decreased production of IL-2 by dephosphorylating the transcriptional enhancer pCREB (16). In subsequent studies we showed that transgenic mice overexpressing PP2Ac in T cells develop glomerulonephritis (25) which was attributed to epigenetic modification of proinflammatory genes (26).

The abundance of PP2A in all cells and the large number of its regulatory subunits (more than 20) point to a complicated landscape whereby PP2A controls cell function (13). Previously, we showed that the PP2A regulatory subunit B β (PPP2R2B) is decreased in SLE T cells and accounts for decreased IL-2 deprivation-induced T-cell apoptosis (19). In this report, we identify that PPP2R2D is overexpressed in T cells from patients with SLE and functions as a negative regulator of IL-2 production in T cells. In addition, under TCR stimulation, PPP2R2D is mostly upregulated whereas PPP2R2B is not affected. Therefore, in T cells two subunits PPP2R2B and PPP2R2D control distinct functions. With regard to the study of T cells from patients with SLE, the involvement of PP2A in the immunopathogenesis of the disease appears to be even more complicated in view of the fact that the expression of PPP2R2B is decreased (20) whereas that of PPP2R2D is increased, as shown in this study.

In this report, we provide evidence that PPP2R2D, in different T cell subsets (T_{conv} and T_{reg}), plays differential essential roles. Upon ATAC-seq, we found that lack of PPP2R2D expression in T_{conv} cells boosts chromatin opening of a large number of genes, while in T_{reg} cells chromatin remodeling is limited. These findings demonstrate that PPP2R2D is more important in the direct regulation of T_{conv} cell function (IL-2 production) rather than T_{reg} cell function. Although silencing PP2Ac or inhibition of its activity increased IL-2 production in T cells (16), in subsequent studies

we found that PP2Ac is requisite for T_{reg} cell function (17) and enables IL-2 signaling during T_{reg} development (18). These apparently contradictory data make PP2Ac inhibitors unlikely to be used for treatment of patients with SLE. Data presented in this study demonstrate clearly that PPP2R2D deficiency enhances the production of IL-2 in T_{conv} cells without directly affecting T_{reg} cells, and thus making PPP2R2D a promising target to treat IL-2-deficient autoimmune and inflammatory disorders. In fact, we present evidence that PPP2R2D deficiency in T cells alleviates imiquimod-induced lupus-like pathology in mice. Our findings are in conceptual agreement with a recent report which demonstrated that T cells with silenced PPP2R2D produced more IL-2 and other cytokines when transferred in to mice along with melanoma cells (27).

IL-2 is produced after antigen activation and is involved in effector responses and immune tolerance (8). On one hand, IL-2 is needed for the expansion of T_{eff} cells (28, 29) and on the other hand, IL-2 drives the development of $CD4^{+}FOXP3^{+}$ regulatory T cells, which have suppressor function and mediate immune tolerance (30, 31). IL-2 consumption by T_{reg} cells has been suggested to be essential for the suppressor function of T_{reg} cells by causing the death of activated T cells (11, 32). Our data from the T_{conv} and T_{reg} cells co-culture experiments showed that PPP2R2D deficiency in T cells potentiates the suppressive function of T_{reg} cells and this is probably due to the fact that more IL-2 is produced by PPP2R2D-deficient T cells. Low-dose IL-2 treatment has been shown to expand T_{reg} cell population in patients with SLE (33, 34), and is used in clinical trials for treatment of autoimmune diseases including SLE, rheumatoid arthritis, and multiple sclerosis (7).

In sum, we have shown that PPP2R2D, a regulatory subunit of PP2A, suppresses the production of IL-2 and T_{reg} cell activity and its specific targeting should increase IL-2 production and T_{reg} activity in autoimmune diseases. Since PPP2R2D is increased in people with SLE, its targeted inhibition should have therapeutic value at least in the subgroup of patients with elevated expression of this subunit. The fact that PP2A is present in every cell and is involved in numerous cell functions, argues for the need to link regulatory subunits to specific cell functions. Patients with autoimmune diseases who have increased levels of PPP2R2D in T cells could benefit from proper inhibitors.

Materials and Methods

Human subjects

Patients who fulfilled the criteria for the diagnosis of systemic lupus erythematosus (SLE) by the American College of Rheumatology were enrolled in this study. This study (Protocol 2006-P-0298) was approved by Beth Israel Deaconess Medical Center (BIDMC) institutional review board. Informed consent was obtained from all study subjects. Age-, sex-, and ethnicity-matched healthy donors were chosen as controls.

Human T cell isolation

The blood from study subjects was incubated for 30 min with a rosette T cell purification kit (Stem Cell Technologies) that contained a tetrameric Ab mixture against CD14, CD16, CD19, CD56, and glyA that attaches non-T cells to erythrocytes. Lymphocyte separation medium (17-829E, Lonza) was subsequently used to separate these complexes from T cells. Cells were then either directly lysed to extract protein and RNA or cultured for following study.

Human T cell culture and stimulation

T cells (1×10^6 to 2.5×10^6) were cultured in RPMI 1640 medium, 10% heat-inactivated FBS, 2 mM glutamine, 100 U/ml penicillin, and 100 μ g/ml streptomycin at 37°C, 5% CO₂. T cells were stimulated with plate bound OKT3/anti-CD3 (5 μ g/ml) and anti-CD28 (1 μ g/ml) for indicated time.

Electroporation in T cells

Control siRNA (Cat# 4404021) and siRNA targeting PPP2R2D (Cat# AM16708) were purchased from Ambion Inc. PPP2R2D plasmid was obtained from Addgene (Plasmid #13804). Plasmid or siRNA electroporation in primary human T cells were carried out using the Nucleofector system (Lonza). Five million freshly isolated T cells were resuspended in 100 μ l of Nucleofector solution and the respective amounts of plasmid or siRNA were added. Cells were transfected using the program U-014 and were rescued immediately in pre-warmed RPMI media supplemented with 10% fetal calf serum and 1% penicillin-streptomycin. Cells were then stimulated using anti-CD3 and anti-CD28 for indicated times and stained for FACS analysis.

Quantitative (q) PCR

Total RNA was isolated from purified T cells with RNAeasy Plus micro kit (QIAGEN). The isolated RNA was transcribed into cDNA using the using the RNA to cDNA premix (Clontech) according to the manufacturer's instructions. SYBR green were purchased from Roche and the assays were performed on 96-well reaction plates (Life Technologies). The real time PCR was performed on StepOnePlus system (Life Technologies). In all experiments β -actin was used as reference gene to normalize gene expression. Primers were shown in Supplemental Table 2.

Flow cytometry

Cells were stained with fluorescence-tagged antibodies purchased from eBioscience, BD Biosciences, Tonbo Bioscience or BioLegend (Supplemental Table 3) and analyzed using Cytotflex flow cytometer. Flow cytometry data were analyzed using CytExpert version 2.0. For intracellular cytokine staining, cells were stimulated with 50 ng/ml of phorbol myristate acetate (PMA), 1 μ M of ionomycin, and 1 μ g/ml of brefeldin A for 4 hours in the presence of brefeldin A, harvested, fixed and stained with BD Cytotfix/Cytoperm Fixation/Permeabilization Solution Kit.

Mice

PPP2R2D flox (R2D^{fl/fl}) mice were generated using CRISPR/Cas9 technology as previously described (21). Briefly, pronuclear zygotes were microinjected with Cas9 protein, two gRNAs targeting intronic regions flanking Exon 6 of PPP2R2D, and donor single-stranded DNA oligonucleotides each containing a loxp consensus sequence and restriction enzyme sites. Litters were crossed with C57BL/6J mice (The Jackson Laboratory) and screened using PCR followed by restriction enzyme digestion to identify candidate founders (R2D^{fl/fl}). Excision of Exon 6 was confirmed by *in vitro* Cre recombination of PCR products amplified from candidate founders. To generate PPP2R2D conditional knock out mice, R2D^{fl/fl} mice were crossed with Lck^{cre} (distal promoter) mice to have Lck^{cre}R2D^{fl/fl} mice where PPP2R2D is deletion in T cells. Both age- and sex-matched male and female mice at the age of 8-12 weeks (unless indicated otherwise in the figure legend) were used for experiments. All mice were bred and housed in a specific pathogen-free environment in a barrier facility in accordance with the Beth Israel Deaconess Medical Center Institutional Animal Care and Use Committee (IACUC).

Induction of lupus-like disease

R2D^{fl/fl} or Lck^{cre}R2D^{fl/fl} mice were received a topical treatment of 1.25 mg of 5% imiquimod cream (Perrigo), a TLR7 stimulator, on the skin of the right ear three times a week from 8 to 16 weeks of age, which induces lupus-like disease as previously described (24). At the end of the experiment, urine, serum, spleen and kidney were collected for indicated analyses respectively.

Enzyme-linked immunosorbent assays (ELISAs)

The amount of albumin and creatinine in urine, as well as serum IgG autoantibody against dsDNA were determined using standardized ELISAs. Following ELISA kits were used: Mouse anti-dsDNA IgG ELISA (Alpha Diagnostic Intl. Inc.); Parameter Creatinine Kit (R&D Systems); and Mouse Albumin ELISA Quantitation Set (Bethyl Laboratories). All procedures were performed according to the manufacturer's instructions.

Single cell isolation

Spleens were excised, weighed and single-cell suspensions were obtained. Kidneys were perfused with PBS and digested with collagenase type IV (300 U/ml, Worthington Biochemical) and DNase I (100 µg/ml, Roche) in Hank's balanced salt solution (HBSS) for 30 min at 37 °C.

Renal histopathology

Histopathologic assessment was performed as previously described (35). Twenty glomeruli per kidney section were evaluated and the average score was calculated in each mouse. The changes of each glomerulus were scored semiquantitatively on a scale of 0-3; 0=normal (30-40 cells per glomerulus), 1=mild (41-50 cells/glomerulus and/or minor exudates), 2=moderate (51-60 cells per glomerulus, hyalinosis and/or moderate exudates) and 3=severe (>60 cells per glomerulus, segmental or global sclerosis, necrosis, crescent formation, and/or heavy exudates).

Complement 3 and IgG staining

Coronal sections of frozen kidneys (6-µm) were fixed, stained with Fluorescein-conjugated goat IgG to mouse complement C3 (MP Biomedicals; 1:100) and Texas-Red goat anti-Mouse IgG Antibody (Invitrogen, 1:100), and mounted with Antifade Mounting Medium with DAPI (Vectashield). Then the images of an entire coronal section were captured with an All-in-One Fluorescence Microscope (BZ-X800E, Keyence) and analyzed using BZ-X800 analyzer. The number of glomeruli with C3 and IgG double deposition in the coronal section of kidney were counted.

Apoptosis detection

Two million of thymocytes were cultured in 96-well plates with 1 µg/mL of anti-CD3 overnight. Then cells were stained with surface antigens (CD4, CD8) at 4 °C for 15 min, washed with cold PBS, and stained with 2 µL of annexin V (BD Pharmingen, 556570) in 200 µL of 1× binding buffer at room temperature for 15 min before being collected for FACS analysis. The FACS data analysis gated on single cell by exclusion of dead cells.

Mouse T cell isolation and culture

Mouse CD4 or CD8 T cells were isolated using EasySep™ Mouse CD4+ (Catalog # 19852) or CD8+ (Catalog # 19853) T Cell Isolation Kit (StemCell Technologies), per manufacturer's instruction. Cell were cultured in RPMI 1640 medium, 10% heat-inactivated FBS, 2 mM glutamine, 100 U/ml penicillin, 100 µg/ml streptomycin, and 2-Mercaptoethanol (50 µM) at 37°C, 5% CO₂.

In vitro T cell differentiation

Naive CD4⁺ T cells were purified by mouse CD4⁺CD62L⁺ T Cell Isolation Kit II (Miltenyi Biotec). Purified naive T cells were stimulated with plate-bound goat anti-hamster antibodies, soluble anti-CD3 (0.25 µg/ml, 145-2C11; Biolegend) and anti-CD28 (0.5 µg/ml, 37.51; Biolegend) for

Th0-non-polarized condition culture. In addition to Th0-non-polarized condition, following stimulation was used for each polarized condition: IL-12 (20 ng/ml; R&D Systems) and anti-IL-4 (10 µg/ml, C17.8; Biolegend) for Th1; IL-6 (3 ng/ml; R&D Systems), TGF-β1 (0.3 ng/ml; R&D Systems), anti-IL-4 (10 µg/ml, C17.8; Biolegend) and anti-IFNγ (10 µg/ml; XMG1.2; Biolegend) for Th17; and IL-2 (20 ng/ml; R&D Systems), TGF-β1 (3 ng/ml), anti-IL-4 (10 µg/ml) and anti-IFNγ (10 µg/ml) for T_{reg}.

In vitro suppression assay

T_{conv} cells (Thy1.2⁺CD4⁺CD25^{lo}CD127^{lo} and Thy1.2⁺CD8⁺CD25^{lo}CD127^{lo}) and T_{reg} (Thy1.2⁺CD4⁺CD25^{hi}CD127^{lo}) cells were sorted from freshly isolated mice splenocytes by FACS Aria II and stained with CellTrace Violet and CFSE, respectively. 4 × 10⁴ T_{conv} cells were cultured with graded numbers of T_{reg} cells in the presence of 1 × 10⁵ irradiated, T cell-depleted splenocytes, and 1 µg/ml anti-CD3 and anti-CD28 in a 96-well round-bottom plate for 72 hours. Cell proliferation of T_{conv} cells was determined by flow cytometry based on the dilution of fluorescence intensity of CellTrace Violet of the gated cells.

Luciferase reporter assay

Mouse IL-2 promoter region (747 bp) was cloned into pGL3-Basic vector by GenScript. R2D^{fl/fl} or Lck^{cre}R2D^{fl/fl} CD4 T cells were nucleofected with IL-2 promoter by using Amaxa Nucleofector electroporation, rested overnight and stimulated with plate bound anti-CD3 (1 µg/ml) and anti-CD28 (1 µg/ml) for 24 hours. Then cells were harvested and lysed, and luciferase activity was detected by GloMax®-Multi Detection System (Promega) using the Dual-Luciferase Reporter Assay Kit (E1910, Promega). Luciferase activity was normalized to renilla luciferase activity as well as to the R2D^{fl/fl} CD4 T cells.

Western blotting

Cell lysates were prepared using RIPA buffer (Boston BioProducts) containing protease cocktail inhibitor (cOMplete Mini EDTA- free, Roche) and phosphatase cocktail inhibitor (Phostop, Roche). Protein concentration was determined by coomassie protein assay reagent (Sigma-Aldrich). Twenty µg of total protein was resolved by a NuPAGE 4-12% Bis-Tris gel (Life Technologies), and transferred to PVDF membrane (Thermo Fisher Scientific). After blocking with 5% non-fat milk (M-0841, LabScientific), the membrane was incubated with primary antibody overnight at 4 °C. Subsequently, the membrane was incubated with secondary antibody for 90 minutes at room temperature. Western ECL substrate (1705061, Bio-Rad) was used to develop the immunoblot. The picture was captured and analyzed by Image Lab (Version 5.2.1) using ChemiDoc™ XRS+ System (Bio-Rad). The results were quantified by plotting the intensity of the band. β-actin was used as the loading control. Primary antibodies against CREB

(#9197) and PP2Ac (#2259) were purchased from Cell Signaling Technology, p-CREB (#06-519) was from Millipore, PPP2R2D (ab181071) was from Abcam, and β -actin (A5316) was from Sigma.

Co-immunoprecipitation

Co-IP experiments were conducted using Pierce™ Classic Magnetic IP/Co-IP Kit (88804, ThermoFisher) according to manufacturer's instructions. Briefly, protein lysates were prepared using ice-cold IP lysis buffer containing protease cocktail inhibitor (cOmplete Mini EDTA- free, Roche). Then antigen/antibody mixture was made by overnight incubation of protein lysate with an antibody either against PP2Ac (#05-421, Millipore), or normal mouse IgG (sc-2025, Santa Cruz Biotechnology) as indicated. Subsequently, the mixture was added to the tube containing pre-washed magnetic beads and incubated for 1 hr at room temperature under continuous mixing. The beads were then collected on a magnetic stand and washed, and the protein complex was eluted from the beads for western blot analysis.

ATAC-seq

ATAC-seq was done as described by Corces et al., (2017). Briefly, R2D^{fl/fl} and Lck^{cre}R2D^{fl/fl} CD4 T_{conv} cells (Thy1.2⁺CD4⁺CD25^{lo}CD127^{lo}), which were sorted out by flow cytometry, were stimulated with plate bound CD3 (1 μ g/ml) and CD28 (1 μ g/ml) antibodies for 4 hours. T_{reg} cells (Thy1.2⁺CD4⁺CD25^{hi}CD127^{lo}), which were sorted out by flow cytometry, were stimulated with IL-2 (20 ng/ml) and plate bound CD3 (1 μ g/ml) and CD28(1 μ g/ml) antibodies for 4 hours. We followed the Omni-ATAC protocol (Corces et al., 2017) and deep sequencing was performed using PE35-bp reads on Illumina NextSeq500 at Boston Nutrition Obesity Research Center Functional Genomics Core.

ATAC-seq data was evaluated for quality using FASTQC. Adapter sequences were trimmed from the raw reads with CutAdapt (v2.7). Trimmed reads of each sample were mapped to the reference house mouse genome build GRCm38 (mm10) by using Bowtie2 (v2.3.5) BAM files were generated and sorted by query name with SAMtools (v1.9). Genrich (v0.6) was used for peak calling using multiple replicates for one condition with default threshold. PCR duplicated reads and reads mapping to mitochondrial DNA and the Y chromosome were filtered. Genomic location of peaks was determined using R package ChIPseeker (v1.22.1). The integrative genomics viewer (IGV) was used to analyze the genomic context of specific differentially accessible regions. Peaks called from ATAC-Seq profiles were annotated using ChIPseeker. In detail, the "TxDb.Mmusculus.UCSC.mm10.knowGene" was used as the annotation database, and the promoter region was defined as \pm 3 kb around the transcriptional start site (TSS). Affinity-based analysis was performed using R package Diffbind (v2.14.0) with the DESeq2

method (V1.26.0). For T_{conv} cells, significant differential peaks were defined as having a $|\log_2$ Fold change $| > 2$ with an adjusted p-value less than or equal to 0.01 in $Lck^{cre}R2D^{fl/fl}$ CD4 T conv cells compared to those in $R2D^{fl/fl}$ CD4 T conv cells. For T_{reg} cells, we used p-value less than or equal to 0.01 as cutoff. TF binding motif analysis of ATAC-seq data was performed using HOMER v4.7.217. Only known motifs from HOMER's motif database were considered. All ATAC-seq data were deposited in the NCBI's Gene Expression Omnibus database (GEO accession no. GSE156927; <https://www.ncbi.nlm.nih.gov/geo/query/acc.cgi?acc=GSE156927>).

Statistics

All statistical analyses were conducted using GraphPad Prism 7 (GraphPad software Inc.). Data were presented as Mean \pm SD. Statistical differences between 2 populations were calculated by t-test (two-tailed) including multiple t-test, unpaired t-test or paired t-test. For multiple populations comparison, two-way ANOVA with Sidak's multiple comparisons test was used. A P value of < 0.05 was considered statistically significant.

Study approval

Human samples study (Protocol 2006-P-0298) was approved by Beth Israel Deaconess Medical Center (BIDMC) institutional review board. All animal procedures were approved by the IACUC of Beth Israel Deaconess Medical Center, Harvard Medical School. All mice were maintained in an SPF animal facility (Beth Israel Deaconess Medical Center). All mice were genotyped to validate claimed strain.

Author contributions

WP designed and performed experiments, analyzed data and wrote the manuscript. AS help to perform the human experiments. AF generated the conditional knockout mice. YZ analyzed the ATAC-seq data. CB and NY help to perform flow cytometry staining and cell sorting. MGT analyzed data, provided critical expertise and edited the manuscript. GCT conceived and supervised the study, interpreted data and wrote the manuscript.

Acknowledgments

The studies were supported by NIH grant AI136924.

References

1. Liu Z, and Davidson A. Taming lupus-a new understanding of pathogenesis is leading to clinical advances. *Nat Med.* 2012;18(6):871-82.
2. Moulton VR, and Tsokos GC. T cell signaling abnormalities contribute to aberrant immune cell function and autoimmunity. *J Clin Invest.* 2015;125(6):2220-7.
3. Tsokos GC. Systemic lupus erythematosus. *N Engl J Med.* 2011;365(22):2110-21.
4. Beringer A, Noack M, and Miossec P. IL-17 in Chronic Inflammation: From Discovery to Targeting. *Trends Mol Med.* 2016;22(3):230-41.
5. Pollard KM, Cauvi DM, Toomey CB, Morris KV, and Kono DH. Interferon-gamma and systemic autoimmunity. *Discov Med.* 2013;16(87):123-31.
6. Rose A, von Spee-Mayer C, Kloke L, Wu K, Kuhl A, Enghard P, et al. IL-2 Therapy Diminishes Renal Inflammation and the Activity of Kidney-Infiltrating CD4+ T Cells in Murine Lupus Nephritis. *Cells.* 2019;8(10).
7. Sharabi A, Tsokos MG, Ding Y, Malek TR, Klatzmann D, and Tsokos GC. Regulatory T cells in the treatment of disease. *Nat Rev Drug Discov.* 2018;17(11):823-44.
8. Liao W, Lin JX, and Leonard WJ. Interleukin-2 at the crossroads of effector responses, tolerance, and immunotherapy. *Immunity.* 2013;38(1):13-25.
9. Kim HP, Imbert J, and Leonard WJ. Both integrated and differential regulation of components of the IL-2/IL-2 receptor system. *Cytokine Growth Factor Rev.* 2006;17(5):349-66.
10. Waldmann TA. The multi-subunit interleukin-2 receptor. *Annu Rev Biochem.* 1989;58:875-911.
11. Chinen T, Kannan AK, Levine AG, Fan X, Klein U, Zheng Y, et al. An essential role for the IL-2 receptor in Treg cell function. *Nat Immunol.* 2016;17(11):1322-33.
12. Ruvolo PP. The broken "Off" switch in cancer signaling: PP2A as a regulator of tumorigenesis, drug resistance, and immune surveillance. *BBA Clin.* 2016;6:87-99.
13. Shi Y. Serine/threonine phosphatases: mechanism through structure. *Cell.* 2009;139(3):468-84.
14. Katsiari CG, Kyttaris VC, Juang YT, and Tsokos GC. Protein phosphatase 2A is a negative regulator of IL-2 production in patients with systemic lupus erythematosus. *J Clin Invest.* 2005;115(11):3193-204. Epub 2005 Oct 13.
15. Sunahori K, Juang YT, Kyttaris VC, and Tsokos GC. Promoter hypomethylation results in increased expression of protein phosphatase 2A in T cells from patients with systemic lupus erythematosus. *J Immunol.* 2011;186(7):4508-17. doi: 10.049/jimmunol.1000340. Epub 2011 Feb 23.
16. Katsiari CG, Kyttaris VC, Juang YT, and Tsokos GC. Protein phosphatase 2A is a negative regulator of IL-2 production in patients with systemic lupus erythematosus. *J Clin Invest.* 2005;115(11):3193-204.
17. Apostolidis SA, Rodriguez-Rodriguez N, Suarez-Fueyo A, Dioufa N, Ozcan E, Crispin JC, et al. Phosphatase PP2A is requisite for the function of regulatory T cells. *Nat Immunol.* 2016;17(5):556-64.
18. Sharabi A, Li H, Kasper IR, Pan W, Meidan E, Tsokos MG, et al. PP2A enables IL-2 signaling by preserving IL-2Rbeta chain expression during Treg development. *JCI Insight.* 2019;5.
19. Crispin JC, Apostolidis SA, Finnell MI, and Tsokos GC. Induction of PP2A Bbeta, a regulator of IL-2 deprivation-induced T-cell apoptosis, is deficient in systemic lupus

- erythematosus. *Proc Natl Acad Sci U S A*. 2011;108(30):12443-8. doi: 10.1073/pnas.1103915108. Epub 2011 Jul 11.
20. Crispin JC, Apostolidis SA, Finnell MI, and Tsokos GC. Induction of PP2A Bbeta, a regulator of IL-2 deprivation-induced T-cell apoptosis, is deficient in systemic lupus erythematosus. *Proc Natl Acad Sci U S A*. 2011;108(30):12443-8.
 21. Yang H, Wang H, Shivalila CS, Cheng AW, Shi L, and Jaenisch R. One-step generation of mice carrying reporter and conditional alleles by CRISPR/Cas-mediated genome engineering. *Cell*. 2013;154(6):1370-9.
 22. Love MI, Huber W, and Anders S. Moderated estimation of fold change and dispersion for RNA-seq data with DESeq2. *Genome Biol*. 2014;15(12):550.
 23. Mayr B, and Montminy M. Transcriptional regulation by the phosphorylation-dependent factor CREB. *Nat Rev Mol Cell Biol*. 2001;2(8):599-609.
 24. Yokogawa M, Takaishi M, Nakajima K, Kamijima R, Fujimoto C, Kataoka S, et al. Epicutaneous application of toll-like receptor 7 agonists leads to systemic autoimmunity in wild-type mice: a new model of systemic Lupus erythematosus. *Arthritis Rheumatol*. 2014;66(3):694-706.
 25. Crispin JC, Apostolidis SA, Rosetti F, Keszei M, Wang N, Terhorst C, et al. Cutting edge: protein phosphatase 2A confers susceptibility to autoimmune disease through an IL-17-dependent mechanism. *J Immunol*. 2012;188(8):3567-71.
 26. Apostolidis SA, Rauen T, Hedrich CM, Tsokos GC, and Crispin JC. Protein phosphatase 2A enables expression of interleukin 17 (IL-17) through chromatin remodeling. *J Biol Chem*. 2013;288(37):26775-84.
 27. Zhou P, Shaffer DR, Alvarez Arias DA, Nakazaki Y, Pos W, Torres AJ, et al. In vivo discovery of immunotherapy targets in the tumour microenvironment. *Nature*. 2014;506(7486):52-7.
 28. Liao W, Lin JX, Wang L, Li P, and Leonard WJ. Modulation of cytokine receptors by IL-2 broadly regulates differentiation into helper T cell lineages. *Nat Immunol*. 2011;12(6):551-9.
 29. Cote-Sierra J, Foucras G, Guo L, Chiodetti L, Young HA, Hu-Li J, et al. Interleukin 2 plays a central role in Th2 differentiation. *Proc Natl Acad Sci U S A*. 2004;101(11):3880-5.
 30. Littman DR, and Rudensky AY. Th17 and regulatory T cells in mediating and restraining inflammation. *Cell*. 2010;140(6):845-58.
 31. Setoguchi R, Hori S, Takahashi T, and Sakaguchi S. Homeostatic maintenance of natural Foxp3(+) CD25(+) CD4(+) regulatory T cells by interleukin (IL)-2 and induction of autoimmune disease by IL-2 neutralization. *J Exp Med*. 2005;201(5):723-35.
 32. Pandiyan P, Zheng L, Ishihara S, Reed J, and Lenardo MJ. CD4+CD25+Foxp3+ regulatory T cells induce cytokine deprivation-mediated apoptosis of effector CD4+ T cells. *Nat Immunol*. 2007;8(12):1353-62.
 33. von Spee-Mayer C, Siegert E, Abdirama D, Rose A, Klaus A, Alexander T, et al. Low-dose interleukin-2 selectively corrects regulatory T cell defects in patients with systemic lupus erythematosus. *Ann Rheum Dis*. 2016;75(7):1407-15.
 34. He J, Zhang X, Wei Y, Sun X, Chen Y, Deng J, et al. Low-dose interleukin-2 treatment selectively modulates CD4(+) T cell subsets in patients with systemic lupus erythematosus. *Nat Med*. 2016;22(9):991-3.
 35. Kikawada E, Lenda DM, and Kelley VR. IL-12 deficiency in MRL-Fas(lpr) mice delays nephritis and intrarenal IFN-gamma expression, and diminishes systemic pathology. *J Immunol*. 2003;170(7):3915-25.

Figures and legends

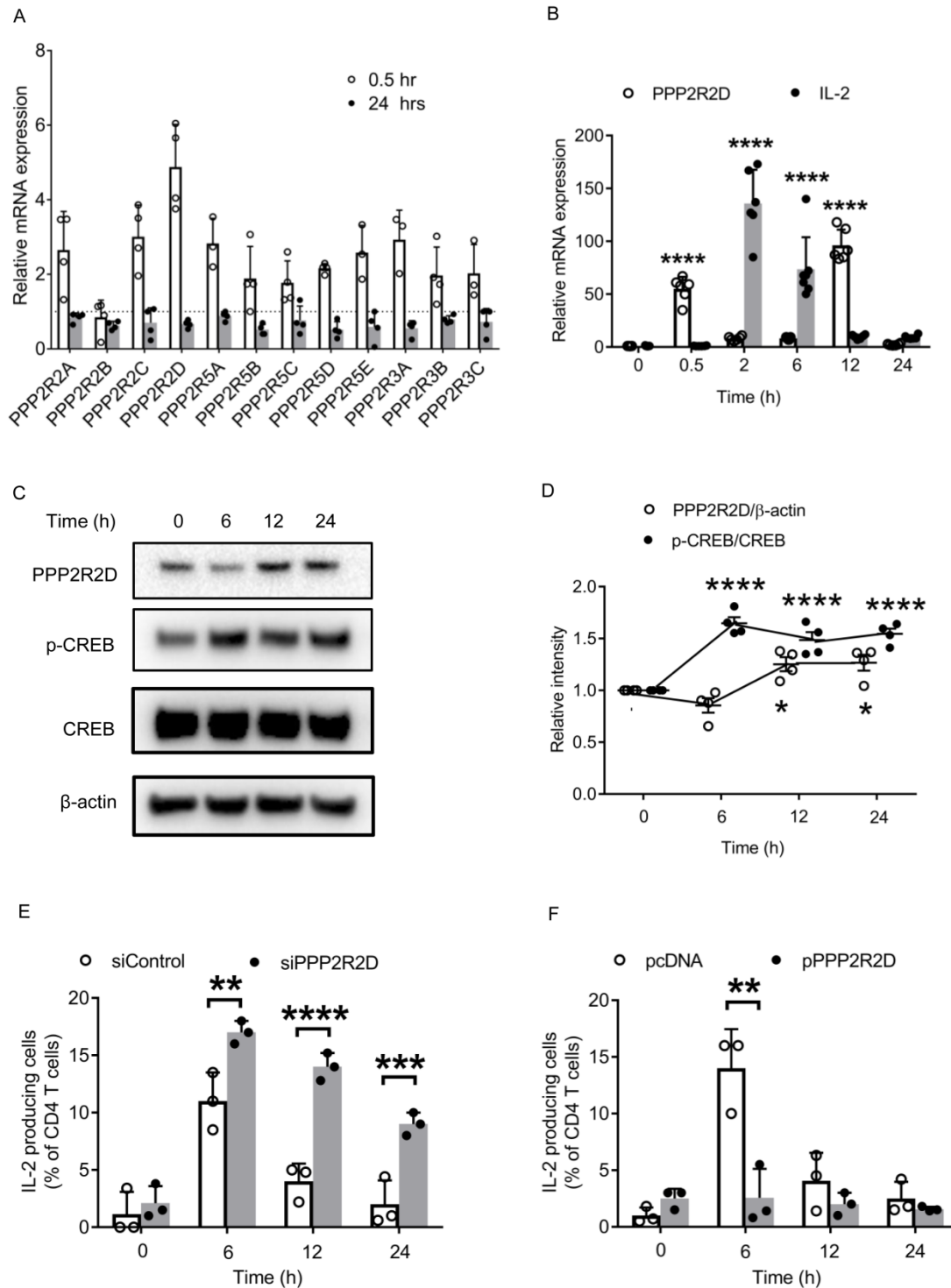


Figure 1. PPP2R2D expression increases and negatively regulates IL-2 production in human T cells following stimulation. Human T cells derived from PBMCs of healthy subjects were stimulated with CD3 (OKT3) and CD28 antibodies. **(A)** The mRNA expression of the

different regulatory subunits of PP2A in T cells at 0.5 and 24 hours post stimulation ($n = 4$). Dashed line represents the expression level of each subunit in T cells without stimulation. **(B)** The mRNA expression of *PPP2R2D* and *IL-2* in T cells at 0, 0.5, 2, 6, 12 and 24 hours post stimulation ($n = 6-7$). All the expression levels were normalized to the samples without stimulation. **(C)** Western blot analysis of protein expression levels of PPP2R2D, p-CREB, CREB and β -actin in T cells at 0, 6, 12 and 24 hours post stimulation. **(D)** Cumulative data ($n = 4$) for quantification of the levels of PPP2R2D and p-CREB in the blots shown in **(C)**. **(E-F)** Intracellular staining of IL-2 production in T cells at 0, 6, 12, and 24 hours post stimulation was analyzed by FACS. Cells were subjected to silencing of PPP2R2D **(E)** or to transfecting with PPP2R2D plasmid **(F)**, and rested overnight before stimulation for indicated time. $n = 3$. **(B)** and **(D)** $*P < 0.05$, $****P < 0.001$, when compared with corresponding 0 hour using Two-way ANOVA with Sidak's multiple comparisons test. **(E)** and **(F)** $**P < 0.01$, $***P < 0.001$, $****P < 0.001$ using Multiple t-test.

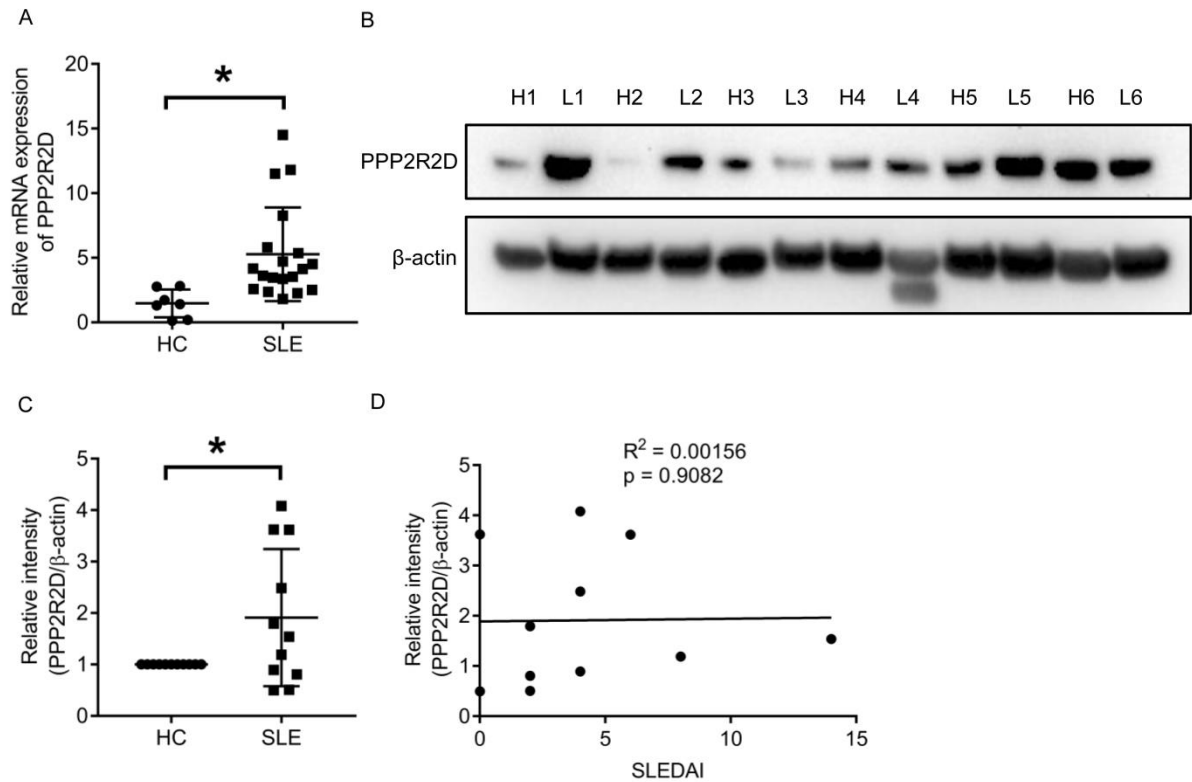


Figure 2. PPP2R2D expression is increased in T cells from patients with SLE. (A) The mRNA expression of *PPP2R2D* and in T cells from healthy subjects ($n = 7$) or from patients with SLE ($n = 19$). HC= Health control. (B) Western blot analysis of the protein expression levels of PPP2R2D and β -actin in T cells from patients with SLE or matched healthy donors. Healthy donor 1 (H1) is age-, sex- and ethnicity-matched with Lupus patient 1 (L1), Healthy donor 2 (H2) is age-, sex- and ethnicity-matched with Lupus patient 2 (L2), and so on. (C) Cumulative data for quantification of the level of PPP2R2D in the blots shown in (B). Health control (HC) ($n = 11$), SLE patients ($n = 11$). (D) Pearson correlation analysis showing the relationship between PPP2R2D expression and Systemic Lupus Erythematosus Disease Activity Index (SLEDAI). * $P < 0.05$ using Unpaired t-test (A) or Paired t-test (C).

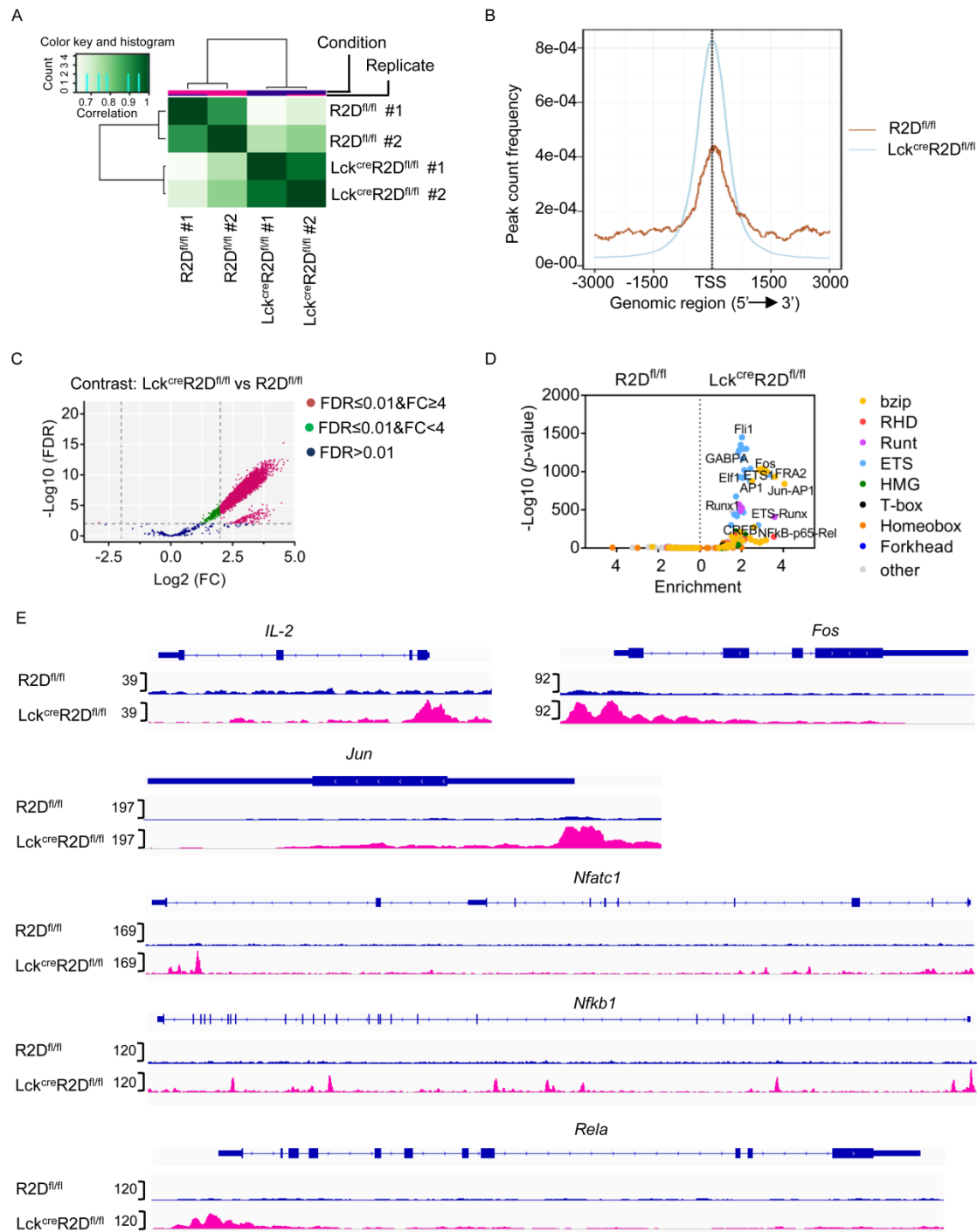


Figure 3. Chromatin accessibility profiles of T_{conv} cells with or without PPP2R2D expression using ATAC-seq analysis. CD4 T_{conv} cells were sorted out from spleens of R2D^{fl/fl} or Lck^{cre}R2D^{fl/fl} mice ($n = 2$ mice/group), and *ex vivo* stimulated by plate bound CD3 and CD28 antibodies for 4 hours before subjected to ATAC-seq. **(A)** Correlation heatmap indicating cross-

correlation between each replicate or each group. **(B)** Histogram showing the distance from the nearest transcription start site (TSS) for all ATAC-seq peaks. **(C)** Volcano plot showing differential chromatin accessibility in CD4 T_{conv} cells isolated from R2D^{fl/fl} (wild-type) and Lck^{cre}R2D^{fl/fl} (knockout) mice. Fold change (FC) is calculated as $\log_2(\text{Lck}^{\text{cre}}\text{R2D}^{\text{fl/fl}} / \text{R2D}^{\text{fl/fl}})$. Red indicates sites that were significantly different (adjusted P value ≤ 0.01 , FC ≥ 4). **(D)** Transcription factor (TF) family binding motifs enriched in loci more accessible in Lck^{cre}R2D^{fl/fl} (Right) or R2D^{fl/fl} (Left) T_{conv} cells; the x axis shows the enrichment factor (ratio of the percentage of differential sites with motifs to the percentage of nondifferential sites with motifs), and the y axis shows the significance level of enrichment. TF families are indicated by color code. **(E)** Accessibility tracks for selected gene loci (*IL-2*, *Fos*, *Jun*, *Nfatc1*, *Nfkb1* and *Rela*) in R2D^{fl/fl} (Up) and Lck^{cre}R2D^{fl/fl} (Down) T_{conv} cells were plotted using the integrative genomics viewer (IGV). ATAC-seq data are average of two biological replicates at each cell type.

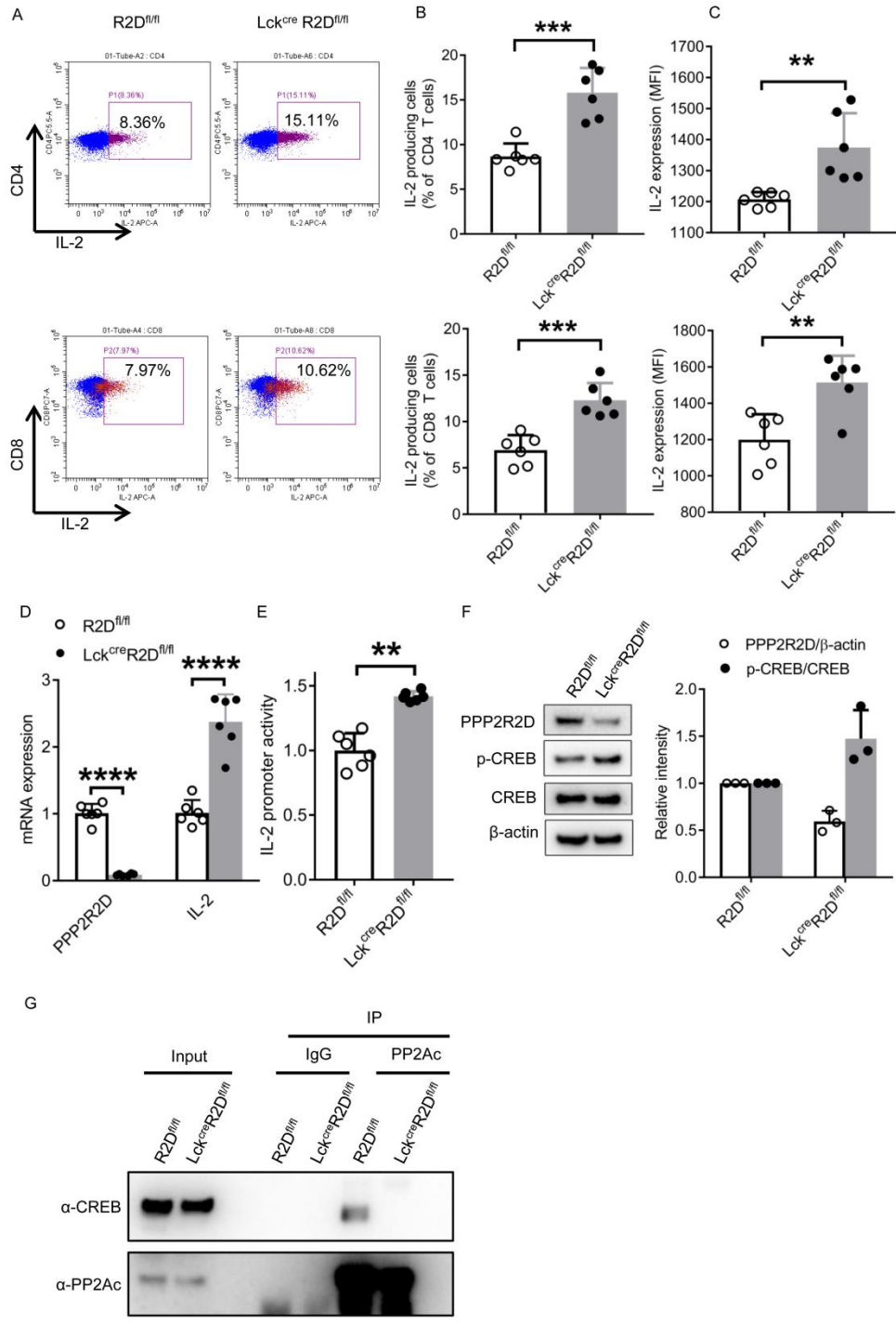


Figure 4. PPP2R2D deficiency enhances IL-2 production by T cells. Splenic CD4 or CD8 T cells were isolated from R2D^{fl/fl} and Lck^{cre}R2D^{fl/fl} mice. **(A-C)** Splenic CD4 or CD8 T cells were stimulated with phorbol myristate acetate (PMA) /ionomycin, and brefeldin A for 4 hours before subjected to fluorescence-activated cell sorting (FACS) analysis of intracellular staining of IL-2 production. Representative flow cytometry plots were shown in **(A)**. Cumulative data ($n =$

6 mice/group) from individual mice depicting the percentages of IL-2-producing cells (**B**) and the expression of IL-2 (**C**) were presented. MFI: mean fluorescence intensity. (**D**) The mRNA expression level of *PPP2R2D* and *IL-2* in R2D^{fl/fl} and Lck^{cre}R2D^{fl/fl} T cells. Splenic CD4 T cells were stimulated with plate bound anti-CD3 and anti-CD28 for 6 hours before extraction of RNA for qPCR analysis. Data are shown as $n = 3$ mice/group with 2 technical replicates for each mouse. (**E**) The promoter activity of IL-2 in R2D^{fl/fl} and Lck^{cre}R2D^{fl/fl} T cells. Splenic CD4 T cells were nucleofected with IL-2 promoter by using Amaxa Nucleofector electroporation, rested overnight and stimulated with plate bound anti-CD3 and anti-CD28 for 24 hours before measurement of luciferase activity. Data are shown as $n = 3$ mice/group with 2 technical replicates for each mouse. (**F-G**) Splenic CD4 T cells were stimulated with plate bound anti-CD3 and anti-CD28 for 6 hours. (**F**) Western blot analysis of PPP2R2D, p-CREB, CREB and β -actin in T cells. Representative immunoblots (left) and cumulative data ($n = 3$ mice/group, right) are presented. (**G**) Co-immunoprecipitation analysis of PP2Ac and CREB in T cells. The blot is representative of three independent experiments. * $P < 0.05$, ** $P < 0.01$, **** $P < 0.001$ using Unpaired t-test.

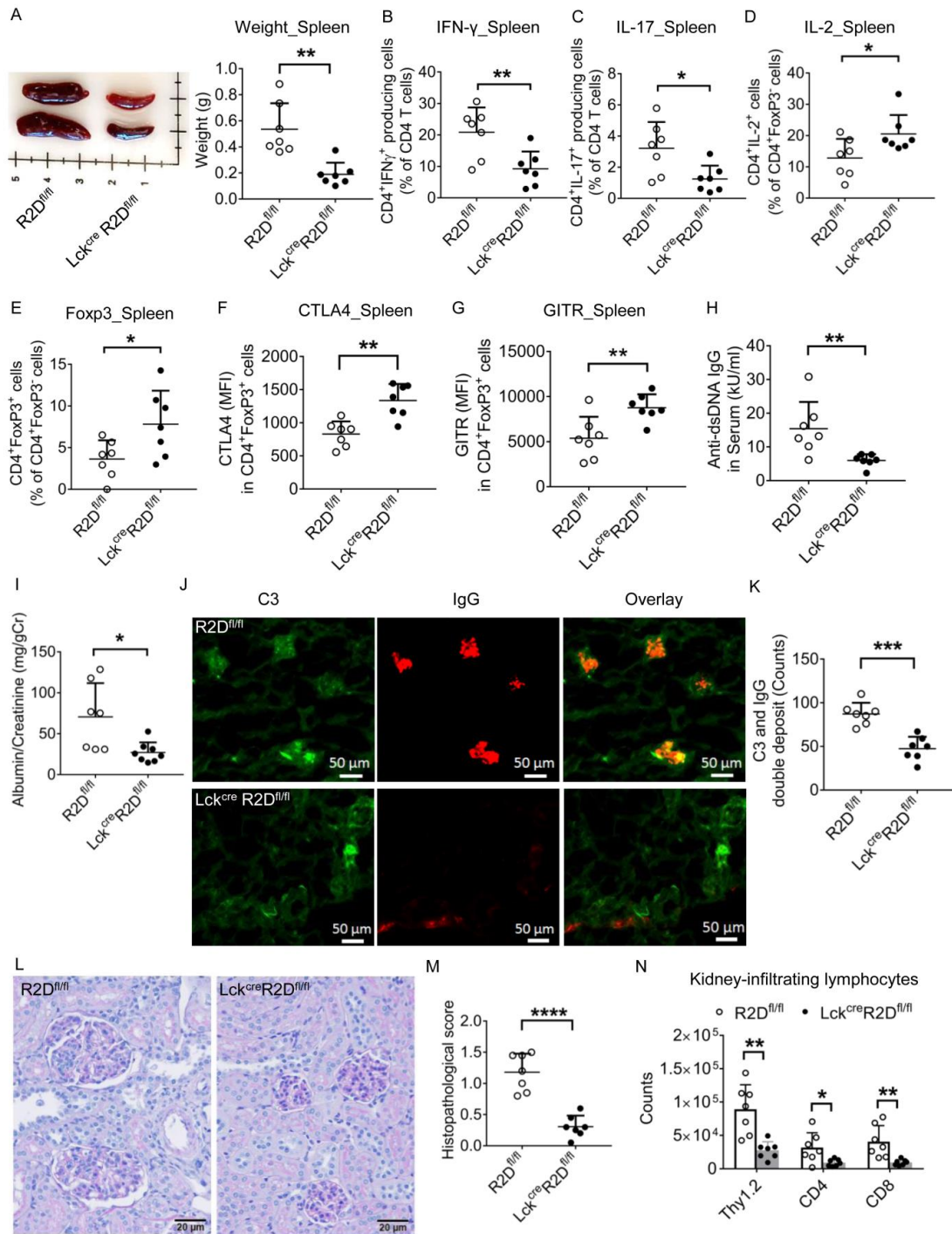


Figure 5. PPP2R2D deficiency in T cells mitigates imiquimod-induced lupus-like pathology in mice. Topical imiquimod was applied to the skin of ear of R2D^{fl/fl} and Lck^{cre}R2D^{fl/fl} mice ($n = 7$ /group) for 8 weeks. **(A)** The representative picture (left) and cumulative data (right) of the weight of spleens. FACS analysis of the percentage of CD3⁺CD4⁺IFN- γ ⁺ **(B)**, CD3⁺CD4⁺IL-17A⁺ **(C)**, CD3⁺CD4⁺IL-2⁺ **(D)** and CD3⁺CD4⁺FoxP3⁺ **(E)** cells in spleens. **(F and G)**

The expression levels of T_{reg} cell markers CTLA-4 (**F**) and GITR (**G**) in splenic T_{reg} (CD3⁺CD4⁺FoxP3⁺) cells were determined by FACS. (**H** and **I**). The anti-dsDNA IgG level in serum (**H**) and the levels of albumin and creatinine in urine (**I**) were measured by ELISA. (**J** and **K**) The deposition of complement 3 (C3) and IgG in glomeruli was determined by immunofluorescence staining. Representative figures (**J**) and cumulative data (**K**) depicting numbers of glomeruli with C3 and IgG double deposition in coronal sections of kidney. Scale bar: 50 μ m. (**L**) Representative H&E staining of kidney tissues. Scale bar: 20 μ m. (**M**) Cumulative data elucidating the histopathologic scores for glomerulonephritis. (**N**) The number of kidney-infiltrating lymphocytes including total T cells (Thy1.2), CD4 and CD8 T cells were counted and analyzed by FACS. * P <0.05, ** P <0.01, **** P <0.001 using Unpaired t-test.

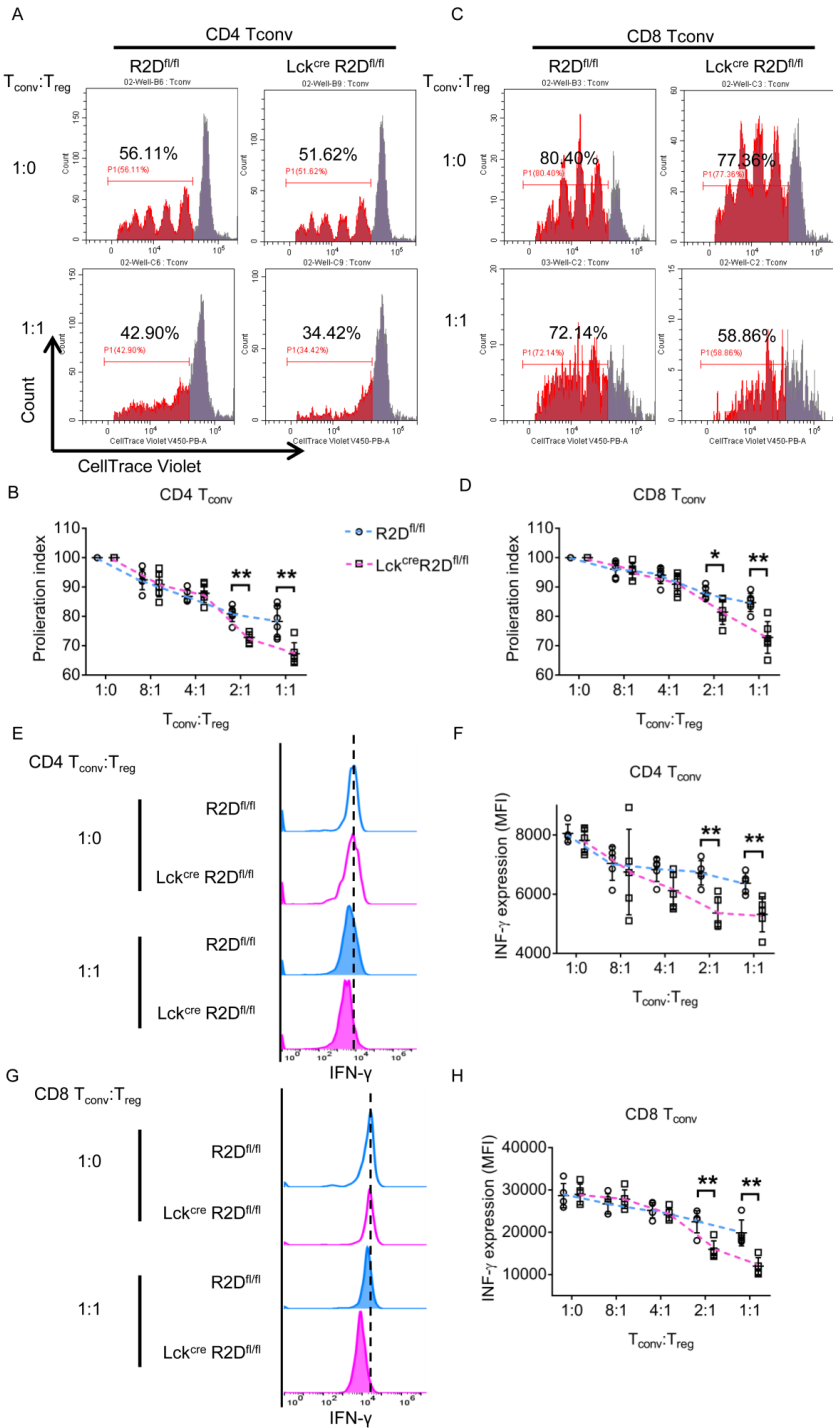


Figure 6. Loss of PPP2R2D expression in T cells enhances the suppressive capacity of T_{reg} cells. *In vitro* suppression of R2D^{fl/fl} or Lck^{cre}R2D^{fl/fl} CD4 T_{conv} or CD8 T_{conv} cells by R2D^{fl/fl} or Lck^{cre}R2D^{fl/fl} T_{reg} cells after incubation together at various ratios. (A-D) Proliferation index of CD4 Tconv (A and B) or CD8 Tconv (C and D) cells is shown. Representative flow charts of the dilution of fluorescent dye CellTrace Violet (A and C) and cumulative data (B and D) are

shown. $n = 6$ mice/group. (**E-H**) Expression of IFN- γ in CD4 Tconv (**E and F**) or CD8 Tconv (**G and H**) cells is shown. Representative flow charts of the expression of IFN- γ (**E and G**) and cumulative data (**F and H**) are shown. $n = 5$ mice/group. * $P < 0.05$, ** $P < 0.01$ using Multiple t-test.

Table 1. Demographic and clinical characteristics of the patients with systemic lupus erythematosus (SLE) and healthy control subjects

	Samples for mRNA		Samples for protein	
	SLE patients (19)	Healthy controls (7)	SLE patients (11)	Healthy controls (11)
Age, mean (range) years	36.8 (23-55)	38.1 (24-55)	40.8 (27-54)	41.8 (27-53)
Sex, no. (%)				
Female	17 (89.5%)	6 (85.7%)	11 (100%)	11 (100%)
Male	2 (10.5)	1 (14.3%)	0	0
Ethnicity, no. (%)				
Caucasian	11 (57.9%)	4 (57.1%)	7 (63.6%)	7 (63.6%)
African American	5 (26.3%)	2 (28.6%)	3 (27.3%)	3 (27.3%)
Asian	3 (15.8%)	1 (14.3%)	0	0
Hispanic	0	0	1 (9.1%)	1 (9.1%)
SLEDAI, mean (range)	3.67 (0-8)	-	4.18 (0-14)	-